Eur. Phys. J. A **13**, 383–397 (2002)

THE EUROPEAN PHYSICAL JOURNAL A

Neutrino-nucleon scattering rate in proto-neutron star matter

L. Mornas[1,a] and A. Pérez[2]

[1] Departamento de Física, Universidad de Oviedo, Av.da Calvo Sotelo, E-33007 Oviedo (Asturias) Spain
[2] Departamento de Física Teórica, Universidad de Valencia, E-46100 Burjassot (Valencia), Spain

Received: 27 June 2001 / Revised version: 14 January 2002
Communicated by V. Vento

Abstract. We present a calculation of the neutrino-nucleon scattering cross-section which takes into account the nuclear correlations in the relativistic random phase approximation (RPA). Our approach is based on a quantum-hadrodynamics model with exchange of σ, ω, π, ρ and δ mesons. In view of applications to neutrino transport in the final stages of supernova explosion and proto-neutron star cooling, we study the evolution of the neutrino mean free path as a function of density, proton-neutron asymmetry and temperature. Special attention was paid to the issues of renormalization of the Dirac sea, residual interactions in the tensor channel, coupling to the delta-meson and meson mixing. In contrast with the results of other authors, we find that the neutral-current process is not sensitive to the strength g' of the residual contact interaction. As a consequence, it is found that RPA corrections with respect to the mean-field approximation amount to only 10% to 15% at high density.

PACS. 26.60.+c Nuclear matter aspects of neutron stars – 13.15.+g Neutrino interactions – 24.10.Jv Relativistic models

1 Introduction

Neutrino transport is a key ingredient to understand the mechanism of supernova explosion and the subsequent cooling of the proto-neutron star formed in the collapse. In the delayed explosion mechanism suggested by Wilson, the problem of shock stall can be overcome if sufficient energy is deposited by the neutrinos to revive the shock. It is seen in recent numerical simulations [1–6] of core collapse that, besides other issues such as convection, the final outcome of the explosion depends sensitively on the rate of neutrino energy deposition.

The following stage of proto-neutron star cooling also depends on the rate of neutrino transport. This determines the shape of the neutrino signal emitted during the first few seconds of the proto-neutron star formation. It has also been suggested that the deleptonization could trigger an instability as the star cools down, and lead to the delayed formation of a black hole, in order to explain the time interval observed between the 8th and 9th neutrino detected in the explosion of the SN1987a supernova. It is thus important to refine the models, since we now begin to benefit from the observation of young-neutron-star surface temperatures, and of the upgrading of neutrino detectors such as SuperKamiokande, SNO or AMANDA (see, *e.g.* [7]) to collect observational data from an eventual supernova explosion.

[a] e-mail: lysiane@pinon.ccu.uniovi.es

An enhanced neutrino emission can occur at high densities if the neutrino-nucleon cross-section is modified through nuclear correlations, as was recognized in the early works of Iwamoto and Pethick [8] and Sawyer [9]. The interest in this topic has recently been revived by the feasibility of full Boltzmann simulations of neutrino transport in collapsing supernovae [2–5].

While early calculations were only taking into account the nucleon mass reduction in the medium, important progress has been realized since then in order to include Hartree-Fock [10], random phase approximation (RPA) [11–17] or ladder [18–24] correlations. It is generally found that the neutrino opacities are suppressed by medium effects, if however no collective modes are excited [16]. As a matter of fact, the latter authors find a sizeable enhancement due to the excitation of a spin zero-sound mode, announcing a transition to a ferromagnetic state in a non-relativistic treatment. Due to the degree of uncertainty existing on the equation of state of neutron star matter at high density, the existence of such a transition remains an open question, although it seems unfavored in a relativistic treatment. Even if no such instability exists, it is important to check the order of magnitude of the suppression factor to be applied to the scattering rate.

In order to asses the importance of some points raised in previous calculations, we present in this paper a new calculation of the neutrino-nucleon rate in dense, hot, asymmetric matter. After a short presentation of the

relativistic meson exchange model and relevant formulae in sect. 2, we first perform a few calculations in a simplified model where the background matter is approximated by pure neutron matter. In particular, we examine the effect of the Dirac sea and of various renormalization procedures commonly used in the literature in order to subtract the divergences in the vacuum fluctuation term. As a matter of fact, calculations reported in [25] ascribed a sizeable correction due to this effect. In contrast, we found here only a minor effect on the size and position of the zero-sound mode in the longitudinal component, which moreover gets washed out by Landau damping and integration over the exchanged momentum and energy. These results are presented in sect. 3.

We also studied the way of introducing the short-ranged residual interaction in the tensor channel, which has to be taken into account in order to avoid the appearance of unobserved pion condensation at low density. In the non-relativistic formalism, this is commonly done by adding a Landau-Migdal contact interaction. In the relativistic case, this has been done by various methods, one being Horowitz's ansatz in the pion propagator [12, 26]. The authors of [13], who are using this ansatz, reported their results to be very sensitive to the choice of the numerical value of the Landau-Migdal constant g'. In the present work, we compare results obtained by this method, to those obtained from a more transparent and straightforward way of introducing this residual interaction through a contact Lagrangian. In contrast with [13], we obtain that the dependence of the neutral current process on the value of g' is extremely weak. We point out a possible explanation for the discrepancy with the authors previously quoted. We argue that the implementation of Horowitz's ansatz introduces additional unphysical contributions, besides the desired corrections to the π and ρ propagators. Once these spurious contributions are properly subtracted, the ansatz of Horowitz would then yield exactly the same results as the contact term Lagrangian. These results are presented in sect. 3.

In a second part of this paper, corresponding to sect. 4, we study the full model where the background matter is asymmetric. The proton fraction may be given as a fixed value, or be determined by β equilibrium in the two extreme situations of neutrino free matter $Y_\nu = 0$, or trapped neutrinos with a lepton fraction typical of supernovae $Y_L \simeq 0.4$. Here we consider with attention the phenomenon of meson mixing, which has not been taken fully into account in some previous treatments. Indeed, in addition to the usual σ-ω mixing, the neutron-proton asymmetry also opens the possibility of σ-ρ and ω-ρ mixing in the case of neutral current relevant for neutrino-nucleon scattering. Finally, we consider here the contribution of the δ-meson. This meson is usually left out, since the σ, ω and ρ mesons are sufficient to describe the properties of nuclear matter at the mean-field level. In asymmetric matter, however, it can have a non-negligible contribution and it mixes with the σ, ω and ρ mesons.

2 Neutrino-nucleon scattering in the relativistic random phase approximation

2.1 Free scattering rate

Two related processes are needed in order to calculate the mean free path and spectrum of neutrinos in matter. They are the neutrino-nucleon scattering through the neutral current

$$\nu(K) + n(P) \rightarrow \nu(K') + n(P')\,, \tag{1}$$

and the absorption (or creation by the inverse process) through the charged current

$$\nu(K) + n(P) \rightarrow e^-(K') + p(P')\,. \tag{2}$$

In either case, the neutrino-nucleon cross-section may be written as

$$\frac{\mathrm{d}\sigma}{\mathrm{d}E_\nu \mathrm{d}\Omega} = \frac{G_\mathrm{F}^2}{64\pi^3}\frac{E_{\nu'}}{E_\nu}\mathcal{I}m(S^{\mu\nu}L_{\mu\nu})\,. \tag{3}$$

We will concentrate in this work on the neutral-current process. Note that we do not include in this definition the Pauli blocking factor for the outgoing lepton. It will be taken into account in the final stage of the calculation, when we compute the mean free path of the neutrino in matter. In this formula, the tensor $L_{\mu\nu}$ represents the lepton current, coupled with the weak vertex $\Gamma^\alpha_{We} = \gamma^\alpha(1-\gamma_5)$. For neutral-current scattering with massless neutrinos, we have

$$L^{\alpha\beta} = \mathrm{Tr}\left[(\gamma\cdot K)\Gamma^\alpha_{We}(\gamma\cdot K')\Gamma^\beta_{We}\right] = 8\big[2K^\alpha K^\beta + (K\cdot q)g^{\alpha\beta} - (K^\alpha q^\beta + q^\alpha K^\beta) \mp i\epsilon^{\alpha\beta\mu\nu}K_\mu q_\nu\big]\,. \tag{4}$$

K and K' are the four-momenta of the ingoing and outgoing leptons. For neutral-current scattering we have $K^2 = K'^2 = 0$. The scattering angle is defined by $\vec{K}\cdot\vec{K'} = E_\nu E'_\nu \cos\theta$. E_ν is the ingoing and $E_{\nu'} = E_\nu - \omega$ is the outgoing lepton energy. The energy loss ω is the zero component of momentum exchange $q^\mu = K^\mu - K'^\mu$.

The structure function can be related to the imaginary part of the retarded polarization

$$S^{\mu\nu}(q) = \int \mathrm{d}^4 x e^{iq\cdot x}\ \langle J^\mu(x)J^\nu(0)\rangle = \tag{5}$$

$$\frac{-2}{1-e^{-z}}\mathcal{I}m\Pi^{\mu\nu}_R \tag{6}$$

and the differential cross-section takes the form

$$\frac{\mathrm{d}\sigma}{\mathrm{d}E_\nu \mathrm{d}\Omega} = -\frac{G_\mathrm{F}^2}{32\pi^3}\frac{E_{\nu'}}{E_\nu}\frac{1}{1-e^{-z}}\mathcal{I}m(\Pi^{\mu\nu}_R L_{\mu\nu})\,. \tag{7}$$

The factor $(1-e^{-z})^{-1}$ with $z = \beta(\omega - \Delta\mu)$ arises from detailed balance. $\Delta\mu$ is the difference between the chemical potential of the outgoing and ingoing nucleons. For the neutral-current process, one has $\Delta\mu = 0$. For the charged-current process, $\Delta\mu = \hat{\mu} = \mu_n - \mu_p$. At the mean-field

level, $\Pi_R^{\alpha\beta}$ is the (retarded) polarization

$$\mathcal{R}e\,\Pi_R^{\alpha\beta} = \mathcal{R}e\,\Pi_{11}^{\alpha\beta}, \qquad \mathcal{I}m\,\Pi_R^{\alpha\beta} = \tanh\left(\frac{\beta\omega}{2}\right)\mathcal{I}m\,\Pi_{11}^{\alpha\beta}\,,$$
$$\Pi_{11}^{\alpha\beta} = -i\int \mathrm{d}^4 p\ \mathrm{Tr}\left[\Gamma^\alpha G^{11}(p)\Gamma^\beta G^{11}(p+q)\right]\,, \tag{8}$$

with Γ^α being the weak vertex of the hadronic current $\Gamma^\alpha = \gamma^\alpha(C_V - C_A\gamma_5)$. For the neutral current, $C_V^n = -1/2$, $C_A^n = -g_A/2$ for the neutron and $C_V^p = 1/2 - 2\sin^2\theta_\mathrm{W}$, $C_A = g_A/2$ for the proton, with $g_A = 1.23$ the axial coupling constant and $\sin^2\theta_\mathrm{W} = 0.232$ is the Weinberg angle. For the charged current we have $C_V = \cos\theta_\mathrm{c}$, $C_A = g_A\cos\theta_\mathrm{c}$, with $\cos\theta_\mathrm{c} = 0.95$ the Cabibbo angle. $G^{11}(p)$ is the nucleon propagator. At the mean-field level, the nucleon behaves as a quasiparticle with effective mass M, momentum P and chemical potential μ, and the propagator can be written as the sum of a vacuum and a density-dependent term (see, *e.g.* [27,28]):

$$G^{11}(p) = (\gamma\cdot P + M)\left\{\frac{1}{P^2 - M^2 + i\epsilon} + 2i\pi\delta(P^2 - M^2)\right.$$
$$\left.\times\left[\theta(p_0)n(p_0) + \theta(-p_0)\overline{n}(p_0)\right]\right\}, \tag{9}$$

with

$$n(p_0) = \frac{1}{e^{\beta(p_0-\mu)}+1}\,, \qquad \overline{n}(p_0) = \frac{1}{e^{-\beta(p_0-\mu)}+1}\,. \tag{10}$$

2.2 RPA corrections

In the hot and dense medium through which the neutrino is moving in the proto-neutron star, the nucleon is not free, but is correlated with the other nucleons through the strong interaction. Several effects contribute, among which are:

- The fact that the nucleons can be described in the medium as quasiparticles with effective masses and chemical potentials. This represents the mean-field approximation. This correction has already been taken into account in the preceding section in the definition of the nucleon propagator.
- One can go a step further and include the exchange term at the level of Hartree-Fock correlations. This is the approach of, *e.g.*, Fabbri and Matera [10]. We will not consider this type of corrections here.
- Another consequence of the correlations is the broadening of the nucleon width, corresponding to the inclusion of ladder corrections [18–20,22]. This is the equivalent for scattering to the Landau-Migdal-Pomeranchuk effect studied in the case of neutrino bremsstrahlung in [23,24,29].
- Finally, one has to take into account the RPA correlations. This is the subject of the present work.

The strong interaction may be modelized by relativistic σ, ω, π and ρ meson exchange. We will also include the δ-meson in a later stage of this calculation (see subsect. 4.1) in order to investigate some specific effects related to the fact that the matter in the proto-neutron star has a sizeable proton-neutron asymmetry. We will work in a relativistic formalism with an interaction Lagrangian of the quantum-hadrodynamics type:

$$\mathcal{L}_\mathrm{int} = \overline{\psi}\Big(-g_\sigma\sigma + g_\omega\gamma^\mu\omega_\mu - \frac{f_\pi}{m_\pi}\gamma_5\gamma^\mu\partial_\mu\vec{\pi}\cdot\vec{\tau}$$
$$-g_\delta\vec{\delta}\cdot\vec{\tau} + g_\rho\gamma^\mu\vec{\rho}_\mu\cdot\vec{\tau} + \frac{f_\rho}{2M}\sigma^{\mu\nu}\partial_\nu\vec{\rho}_\mu\cdot\vec{\tau}\Big)\psi$$
$$-\frac{1}{3}bm_N(g_\sigma\sigma)^3 - \frac{1}{4}c(g_\sigma\sigma)^4\,. \tag{11}$$

The coupling of the pion is taken in the pseudovector form, since this is known to reproduce better the phenomenology of nucleon-pion scattering. It will be seen anyway, at the end of the calculation, that in fact the pion does not contribute directly to the neutral-current process. The non-linear σ couplings σ^3, σ^4 are introduced in order to obtain a better description of the equation of state with a value of the incompressibility modulus and effective mass at saturation density in agreement with the experimental data.

RPA correlations can be introduced by substituting the mean-field polarization in eq. (7) by the solution of the Dyson equation

$$\widetilde{\Pi}_{WW}^{\mu\nu} = \Pi_{WW}^{\mu\nu} + \sum_{a,b=\sigma,\omega,\rho,\pi\ldots} \Pi_{WS}^{(a)\,\mu\alpha} D_{SS\,\alpha\beta}^{(ab)} \widetilde{\Pi}_{SW}^{(b)\,\beta\nu}\,, \tag{12}$$

where the index W stands for a vertex with a weak coupling and S for a vertex with a strong coupling. The tilde $\widetilde{\Pi}$ indicates a resummed polarization. D_{SS} is the propagator of the mesons $a = \sigma,\ \omega,\ \rho^0, \pi^0$ for the neutral-current process (we will see later that the pion does not contribute) or $a = \rho^\pm,\ \pi^\pm$ for the charged-current process. The first term of the Dyson equation corresponds to the mean-field approximation taken in the preceding section.

The Dyson equation can be rewritten as

$$\widetilde{\Pi}_{WW}^{\mu\nu} = \Pi_{WW}^{\mu\nu} + \sum_{a,b=\sigma,\omega,\rho,\pi\ldots} \Pi_{WS}^{(a)\,\mu\alpha} \widetilde{D}_{SS\,\alpha\beta}^{(ab)} \Pi_{SW}^{(b)\,\beta\nu}\,, \tag{13}$$

which provides a solution in terms of the meson propagator $\widetilde{D}_{SS}$ dressed in the RPA approximation.

2.3 Polarizations

Polarization insertions were calculated in the relativistic random phase approximation. They are given by the loop integral

$$\Pi^{AB} = -i\int \frac{\mathrm{d}^4 p}{(2\pi)^4}\mathrm{Tr}\left[\Gamma^A G(p)\Gamma^B G(p+q)\right]\,. \tag{14}$$

$G(p)$ is the nucleon propagator calculated in the Hartree approximation, as given in eq. (9). The Γ^A are the vertices

of the interaction, which can be either of the weak type $\Gamma_W = C_V\gamma^\mu + C_A\gamma_5\gamma^\mu$ or of the strong type Γ_S with $S = \{\sigma, \omega, \rho, \pi, \delta\}$. Formulae are given for the polarizations in, *e.g.*, [12,30–33].

The polarizations can also be obtained by performing a linear response analysis on a Hartree ground state. This was the method used in the following references, to which the reader is referred for a full account of the calculation techniques and meson dispersion relations. The method was described in [34–40], with results given for the π-meson in [34], for the σ, and ω mesons in [35,36] and for the ρ in [37,38].

The linear response analysis provides us with a set of coupled homogeneous equations in the form $\mathrm{Disp}(q)\phi_1(q) = 0$, where $\phi_1(q)$ is a vector formed by the components of the perturbations to the various meson fields, and $\mathrm{Disp}(q)$ is a matrix whose determinant yields the dispersion relation(s). The matrix of dressed meson propagators $\widetilde{D}^{(ab)}_{SS\,\alpha\beta}$, which appear in the second formulation of the weak polarization RPA eq. (13), is then equal to the inverse of this dispersion matrix. The necessary corrections arising from the presence of the non-linear σ^3 and σ^4 couplings automatically appear during the derivation; it is observed (see, *e.g.* eq. (26) of [40]) that they act as a modification to the σ-meson mass by a term $2bm\sigma_H + 3c\sigma_H^2$, where σ_H is the mean-field value of the sigma condensate.

The notation we are using here can be found in [39], which also presents a discussion of some results concerning the introduction of the contact term. Results concerning asymmetric matter are presented in [40]. A new feature is here the mixing between mesons of different isospin when the distribution functions of the protons and neutrons differ. As a consequence, the Dyson equation (13) acquires a more complex structure. The formulae needed for the calculation of the mixed polarizations and meson propagators are too long to be reproduced here; they were given in [40].

The polarizations calculated in the linear response analysis coincide with those available in the literature from the Green function formalism at zero temperature and in symmetric nuclear matter. At finite temperature, the real parts coincide, but some precisions are necessary concerning the imaginary parts. In the real-time formalism [28], one defines the Green function and self-energies as 2×2 matrices, with the indices labeling the two branches of the time contour. The various components are related to each other. In this paper, we chose to work with the retarded polarization.

Polarizations are generally obtained under the form of a "density dependent" and a "vacuum fluctuation" term. This latter part entails divergences which have to be subtracted by some renormalization procedure. Regularization of divergences occurring in the vacuum polarization may be performed through the inclusion of a counterterm Lagrangian with couplings adjusted so as to cancel the infinities. The subtraction is defined up to some residual finite constant, which is then determined by choosing a renormalization point where the polarization and its derivatives with respect to the momentum and effective mass is required to vanish.

The criteria guiding this choice will have to be reexamined in the light of the recent advances concerning effective field theories. As a matter of fact, the various possible renormalization schemes unfortunately lead to discrepancies observed among the results available in the literature. A particularly distressing example was the case of the ρ-meson discussed in [38]. One cannot ignore the problem, since simply eliminating the vacuum by a normal reordering produces pathologies in the dispersion relation. The problem roots in the fact that we are working with an effective theory, which is non-renormalizable in the usual QED sense. A renormalization can still be performed at a given order. Nevertheless, the parameters of the theory, which are adjusted so as to reproduce available experimental data, should enforce the symmetries and scalings of the integrated degrees of freedom of the underlying more fundamental theory. There is some hope that one could solve the problem using "naturalness" arguments [41]. Fortunately, as we will see in sect. 3, our final result has only a negligibly weak dependence in the choice of the renormalization condition.

The polarization which enters in the definition of the differential neutrino-nucleon scattering cross-section may be decomposed onto orthogonal projectors, formed with the vectors and tensor available in the problem, *i.e.* the metric $g^{\mu\nu} = \mathrm{diag}\,(1,-1,-1,-1)$, the hydrodynamic velocity u^μ and the transferred momentum q^μ:

$$\widetilde{\Pi}^{\mu\nu}_{WW} = \widetilde{\Pi}_T\ T^{\mu\nu} + \widetilde{\Pi}_L\ \Lambda^{\mu\nu} + \widetilde{\Pi}_Q\ Q^{\mu\nu} + i\,\widetilde{\Pi}_E\ E^{\mu\nu}\,, \quad (15)$$

with

$$\begin{aligned}
\Lambda^{\mu\nu} &= \frac{\eta^\mu\eta^\nu}{\eta^2}\,, \qquad \eta^\mu = u^\mu - \frac{q\cdot u}{q^2}q^\mu\,,\\
T^{\mu\nu} &= g^{\mu\nu} - \frac{\eta^\mu\eta^\nu}{\eta^2} - \frac{q^\mu q^\nu}{q^2}\,,\\
E^{\mu\nu} &= \epsilon^{\mu\nu\rho\lambda}\eta_\rho q_\lambda\,,\\
Q^{\mu\nu} &= \frac{q^\mu q^\nu}{q^2}\,. \qquad (16)
\end{aligned}$$

The imaginary unit i appearing before the antisymmetric tensor $E^{\mu\nu}$ combines with the i present in the corresponding term of the lepton current, so that the product involves the imaginary part of the polarization Π_E. The following properties might be useful:

$$\begin{aligned}
&T^{\mu\alpha}Q_\alpha{}^\nu = T^{\mu\alpha}\Lambda_\alpha{}^\nu = \Lambda^{\mu\alpha}Q_\alpha{}^\nu = \Lambda^{\mu\alpha}E_\alpha{}^\nu = E^{\mu\alpha}Q_\alpha{}^\nu = 0\,,\\
&\Lambda^{\mu\alpha}\Lambda_\alpha{}^\nu = \Lambda^{\mu\nu}, \qquad Q^{\mu\alpha}Q_\alpha{}^\nu = Q^{\mu\nu}, \qquad T^{\mu\alpha}T_\alpha{}^\nu = T^{\mu\nu}\,,\\
&E^{\mu\alpha}T_\alpha{}^\nu = E^{\mu\nu}, \qquad E^{\mu\alpha}E_\alpha{}^\nu = q^2\eta^2 T^{\mu\nu}\,. \qquad (17)
\end{aligned}$$

When calculating the polarization of the mesons with formula (14), a zero-sound branch appears in the dispersion relation of the pion. Even though it is weaker than in the non-relativistic formulation, it remains a spurious effect, since no such effect is observed experimentally. When analyzing the structure of the pion potential,

it is seen that this is related to the short-range behavior. The introduction of the short-range effects actually should come out of a full many-body calculation. Nevertheless, it is a common practice to implement it by the introduction of a residual interaction. In the non-relativistic formalism, one adds the Landau-Migdal contact interaction $V_C = g'(f_\pi/m_\pi)^2\delta(r)\sigma_1\cdot\sigma_2$. In the relativistic case, several ansätze have been suggested.

For example, Horowitz *el al.* [12,26] modify the free pion propagator as follows:

$$\frac{1}{q^2-m_\pi^2} \longrightarrow G_\pi^{(0)\mu\nu} = \frac{q^\mu q^\nu}{q^2-m_\pi^2} - g' g^{\mu\nu} \tag{18}$$

and obtain the pion and rho propagators dressed at the RPA level by inverting $G^{-1} = G_0^{-1} - \Pi^{-1}$, *i.e.* explicitly,

$$\begin{bmatrix} G_\rho^{\mu\nu} & G_{\rho\pi}^{\nu} \\ G_{\pi\rho}^{\mu} & G_\pi^{\mu\nu} \end{bmatrix}^{-1} = \begin{bmatrix} G_\rho^{(0)\mu\nu} & 0 \\ 0 & G_\pi^{(0)\mu\nu} \end{bmatrix}^{-1} - \begin{bmatrix} \Pi_\rho^{\mu\nu} & \Pi_{\rho\pi}^{\mu\nu} \\ \Pi_{\pi\rho}^{\mu\nu} & \Pi_\pi^{\mu\nu} \end{bmatrix}^{-1} . \tag{19}$$

In these expressions, the polarizations $\Pi_{\pi\rho}^{\mu}$ and $\Pi_\pi^{\mu\nu}$ are calculated with a pseudo*vector* "pion" vertex $(f_\pi/m_\pi)\gamma_5\gamma^\mu$. The true pion is obtained by projecting over q_μ.

In other words, when the dressed "pion" propagator $G_\pi^{\mu\nu}$ is decomposed with the help of the projectors (16)

$$G_\pi^{\mu\nu} = -G_{\pi\,L}\Lambda^{\mu\nu} - G_{\pi\,T}T^{\mu\nu} - G_{\pi\,Q}Q^{\mu\nu}$$

only the component $G_{\pi\,Q}$ is physically meaningful. The $G_{\pi\,L}$ and $G_{\pi\,T}$ components, characteristic of a vector meson, are spurious, and should be removed carefully before proceeding onward with the calculation. As a matter of fact, it was obtained in [39] that these pieces would strongly affect the propagation in the spacelike region, and could even give spurious branches depending on the values of the coupling and cutoff parameters. The same remark applies to the mixed $G_{\rho\pi}^{\nu}$ propagator which is also orthogonal to q^μ and should be removed in later stages of the calculation.

Another more conventional possibility is to add a contact term to the Lagrangian

$$\mathcal{L} \ni g'\left(\frac{f_\pi}{m_\pi}\right)^2 \left(\overline{\psi}\gamma_5\gamma_\mu\psi\right)\left(\overline{\psi}\gamma_5\gamma^\mu\psi\right) . \tag{20}$$

When the dispersion relations of the mesons are calculated using the method of linear response analysis on the Hartree ground state, this leads to self-consistent equations for the pion and rho polarizations [39] whose solution is given by (21),(22). A detailed derivation of these expressions can be found in [39].

Both alternatives modify the polarization of the (true) pion and of the transverse mode of the ρ-meson as follows:

$$\Pi_\pi \longrightarrow \frac{q^2\Pi_\pi}{q^2 - g'\Pi_\pi} , \tag{21}$$

$$\Pi_{\rho T} \longrightarrow \Pi_{\rho T} - \frac{\eta^2 q^2 g' \Pi_{\rho\pi}^2}{1 + g'\Pi_{\pi T}} , \tag{22}$$

with

$$\Pi_{\pi T} = -\frac{1}{2}\Pi_\pi^{\mu\nu}T_{\mu\nu} ,$$

and

$$\eta^2 q^2 \Pi_{\pi\rho} = -\frac{1}{2}\Pi_{\pi\rho}^{\mu\nu}E_{\mu\nu} .$$

We wish to stress the fact that *both* ansätze lead to analytically identical expressions for the dressed pion and transverse rho propagators $G_{\pi Q}$ and $G_{\rho\,T}$, so that results concerning, *e.g.*, the Gamow-Teller resonance, or the longitudinal-to-transverse spin-transfer ratio in $(\vec{p},\vec{n})$ scattering experiments, will not be affected by the way the contact term was introduced. However, the first procedure presents the drawback of introducing additional terms in the dispersion relation, related to the unphysical components of the auxiliary "pion". We feel that the second procedure is more transparent. It can also easily be extended to the case $g'_\rho \neq g'_\pi$ considered, *e.g.*, in [42], by introducing an additional piece to the contact Lagrangian. Since, as will be seen in the next section, we obtain that the neutral-current process is insensitive to the numerical value of g', we will not pursue this line here. On the other hand, it can be expected that the charged-current reaction will be sensitive to the strength of the residual interaction. One might then need to enforce this distinction in order to be consistent with the experimental data available so far.

3 Preliminary study in pure neutron matter

The RPA correction to the mean-field value of the polarization entering the definition of the neutrino-nucleon differential scattering cross-section is

$$\Delta\Pi_{\rm RPA}^{\mu\nu} = \begin{pmatrix} \Pi_{WS}^{(\sigma)\mu} & \Pi_{WS}^{(\omega)\mu\alpha} & \Pi_{WS}^{(\rho)\mu\alpha} & \Pi_{WS}^{(\pi)\mu} \end{pmatrix} \times \begin{pmatrix} G^{(\sigma)} & G_\beta^{\sigma\omega} & 0 & 0 \\ G_\alpha^{(\omega\sigma)} & G_{\alpha\beta}^{(\omega)} & 0 & 0 \\ 0 & 0 & G_{\alpha\beta}^{(\rho)} & 0 \\ 0 & 0 & 0 & G^{(\pi)} \end{pmatrix} \begin{pmatrix} \Pi_{SW}^{(\sigma)\nu} \\ \Pi_{SW}^{(\omega)\beta\nu} \\ \Pi_{SW}^{(\rho)\beta\nu} \\ \Pi_{SW}^{(\pi)\nu} \end{pmatrix} = \Delta\Pi_{\rm RPA}^{L}\Lambda^{\mu\nu} + \Delta\Pi_{\rm RPA}^{T}T^{\mu\nu} + \Delta\Pi_{\rm RPA}^{Q}Q^{\mu\nu} + i\Delta\Pi_{\rm RPA}^{E}E^{\mu\nu} . \tag{23}$$

By introducing the decomposition of the polarizations and propagators onto the projection tensors (16), we obtain (where we have dropped the "WS" index indicating that the polarization loops connect a weak vertex with a strong one)

$$\Delta\Pi_{\rm RPA}^{L} = \Pi_\sigma G_\sigma \Pi_\sigma \eta^2 + 2\,\Pi_\sigma G_{\sigma\omega}\Pi_{\omega\,L}\eta^2 - \Pi_{\omega\,L}G_{\omega\,L}\Pi_{\omega\,L} - \Pi_{\rho\,L}G_{\rho\,L}\Pi_{\rho\,L} , \tag{24}$$

$$\Delta\Pi_{\rm RPA}^{T} = -\Pi_{\omega\,T}G_{\omega\,T}\Pi_{\omega\,T} + \Pi_{\omega\,E}G_{\omega\,T}\Pi_{\omega\,E}\eta^2 q^2 - \Pi_{\rho\,T}G_{\rho\,T}\Pi_{\rho\,T} + \Pi_{\rho\,E}G_{\rho\,T}\Pi_{\rho\,E}\eta^2 q^2 , \tag{25}$$

$$\Delta\Pi_{\rm RPA}^{E} = -2\,\Pi_{\omega\,T}G_{\omega\,T}\Pi_{\omega\,E} - 2\,\Pi_{\rho\,T}G_{\rho\,T}\Pi_{\rho\,E} , \tag{26}$$

$$\Delta\Pi_{\rm RPA}^{Q} = -\Pi_\pi G_\pi \Pi_\pi , \tag{27}$$

$\Delta\Pi^{\mu\nu}_{\rm RPA}$ must now be contracted with the tensor of the lepton current $L_{\mu\nu}$. Using the property

$$L^{\mu\nu}Q_{\mu\nu} = 0\,, \tag{28}$$

we can see that the pion does not contribute to the neutrino-nucleon scattering. The contact term g' contributes indirectly, by modifying the transverse rho propagator $G_{\rho T}$ according to eq. (22). This dependence is nor very strong, since the ρ-meson propagator was already well-behaved in this zone.

In contrast, if the vector components of the auxiliary pion were kept at this stage of the calculation, they would contribute additional pieces to the transverse and longitudinal polarizations

$$\begin{aligned}
\Delta\Pi^{L}_{\rm RPA} &\leftarrow -\Pi_{\pi\,L}G_{\pi\,L}\Pi_{\pi\,L}\,,\\
\Delta\Pi^{T}_{\rm RPA} &\leftarrow -\Pi_{\pi\,T}G_{\pi\,T}\Pi_{\pi\,T} + \Pi_{\pi\,E}G_{\pi\,T}\Pi_{\pi\,E}\,\eta^2q^2\\
&\quad +2\;\Pi_{\rho\,T}G_{\pi\rho}\Pi_{\pi\,E}\,\eta^2q^2 + 2\;\Pi_{\rho\,E}G_{\pi\rho}\Pi_{\pi\,T}\,\eta^2q^2\,,\\
\Delta\Pi^{E}_{\rm RPA} &\leftarrow -2\;\Pi_{\pi\,T}G_{\pi\,T}\Pi_{\pi\,E} - 2\;\Pi_{\pi\,T}G_{\pi\rho}\Pi_{\rho\,T}\\
&\quad +2\;\Pi_{\pi\,E}G_{\pi\rho}\Pi_{\rho\,E}\,\eta^2q^2\,.
\end{aligned}$$

The propagators $G_{\pi\,L}$, $G_{\pi\,T}$ and $G_{\pi\rho}$ vanish when $g' = 0$. On the other hand, when $g' \neq 0$, we observed from our numerical results, that the contribution of these pieces would rapidly become dominant. According to the discussion presented at the end of the previous section, these terms are unphysical and should be removed.

It also appears reasonable that the dependence on the contact term should remain weak, since these term was introduced in order to correct the behavior of the pion, whereas, according to (27) together with (28), the pion does not contribute at lowest order.

3.1 Response functions

The contraction of the lepton current with the polarization can be expressed by means of three structure functions $R_1(q)$, $R_2(q)$ and $R_5(q)$ defined as follows [17]:

$$\begin{aligned}
S^{\mu\nu}(q) = \int \mathrm{d}^4\,x e^{iq.x}\;\langle J^\mu(x)J^\nu(0)\rangle &= R_1(q)u^\mu u^\nu\\
&+R_2(q)(u^\mu u^\nu - g^{\mu\nu}) + R_3(q)q^\mu q^\nu\\
&+R_4(q^\mu u^\nu + q^\mu u^\nu) + iR_5(q)\epsilon^{\mu\nu\alpha\beta}\eta_\alpha q_\beta\,.
\end{aligned} \tag{29}$$

Using the properties

$$\begin{aligned}
&L^{00} = 8E_\nu(E_\nu - \omega)(\cos\theta + 1)\,,\\
&L^{\mu\nu}g_{\mu\nu} = 16K\cdot q = 16E_\nu E'_\nu(\cos\theta - 1)\,,
\end{aligned} \tag{30}$$

$$L^{\mu\nu}\Lambda_{\mu\nu} = \frac{-q^2}{k^2}L^{00} = -\frac{q^2}{k^2}8E_\nu E'_\nu(\cos\theta + 1)\,, \tag{31}$$

$$L^{\mu\nu}T_{\mu\nu} = 8q^2 + \frac{q^2}{k^2}L^{00} = \frac{q^2}{k^2}\left[8\omega^2 + 8E_\nu E'_\nu(3-\cos\theta)\right], \tag{32}$$

$$E^{\mu\nu}L_{\mu\nu} = 8q^2(E_\nu + E'_\nu)\,, \tag{33}$$

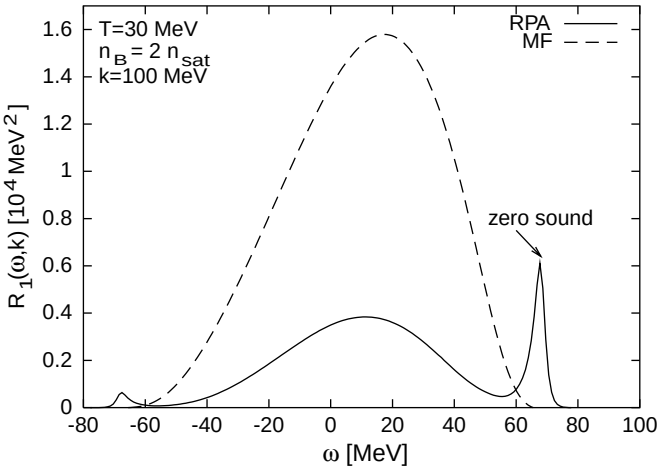

Fig. 1. Structure function R_1, displaying overall RPA reduction and zero-sound enhancement.

we arrive at

$$\begin{aligned}
-2\frac{\mathcal{I}m\left(L^{\mu\nu}\Pi^R_{\mu\nu}\right)}{1-e^{-z}} = 4E_\nu E_{\nu'}[R_1(1+\cos\theta) + R_2(3-\cos\theta)\\
-2(E_\nu + E_{\nu'})R_5(1-\cos\theta)]\,.
\end{aligned} \tag{34}$$

The structure functions are related to the previous polarizations $\Pi^{\mu\nu} = \Pi^{\mu\nu}_{\rm MF} + \Delta\Pi^{\mu\nu}_{\rm RPA} = \Pi_L\,\Lambda^{\mu\nu} + \Pi_T\,T^{\mu\nu} + \Pi_Q\,Q^{\mu\nu} + i\,\Pi_E\,E^{\mu\nu}$ by

$$R_1 = \frac{-2}{1-e^{-z}}\;\mathcal{I}m\left[-\frac{q^2}{\mathbf{q}^2}\Pi_L + \frac{w^2}{\mathbf{q}^2}\Pi_T\right], \tag{35}$$

$$R_2 = \frac{2}{1-e^{-z}}\;\mathcal{I}m\left[\Pi_T\right], \tag{36}$$

$$R_5 = \frac{2}{1-e^{-z}}\;\mathcal{I}m\left[\Pi_E\right]. \tag{37}$$

In the non-relativistic limit, R_1 and R_2 reduce to the density and spin density correlation functions, respectively. The axial-vector structure function R_5 appears only in a relativistic treatment.

The "vector" structure function R_1 involves the sigma-meson and the longitudinal part of the omega-meson, as well as the longitudinal part of the rho. The contribution of the latter meson is negligible in this channel. As is known from previous studies, a zero-sound mode appears in the mixed σ-ω dispersion relation. It manifests itself as a pole in the RPA meson propagator. At finite temperature, it is quenched by Landau damping. As an example, the longitudinal response function is represented in fig. 1 at twice the saturation density and a temperature $T = 30$ MeV for a fixed exchanged 3-momentum $k = 100$ MeV. The longitudinal response function is suppressed in the RPA approximation (full line) as compared to the mean-field approximation (dashed line). The zero sound appears as a peak at the high-frequency edge of the distribution strength. Note, however, that this mode will lie mostly outside of the integration range when we calculate the mean free path. Indeed, the fact that the exchanged momentum must be spacelike restricts the frequency to

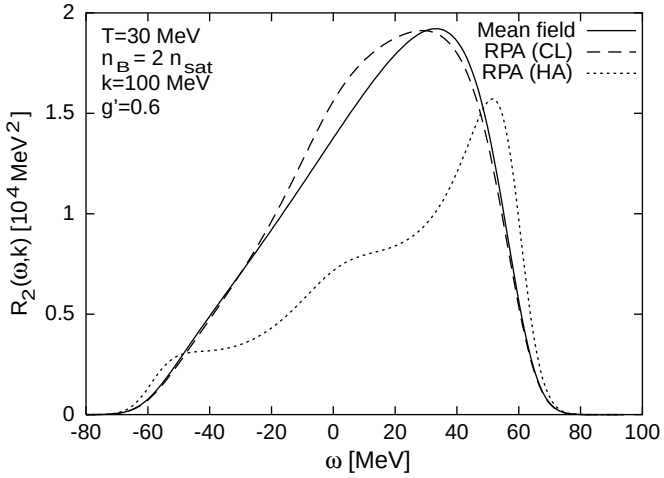

Fig. 2. Structure function R_2, with two ways of implementing the short-range correlations parametrized by Landau-Migdal parameter g'. In the curve (HA), the auxiliary unphysical components of the pion were kept. If these components are removed by hand, the results of Horowitz's ansatz would coincide with those of the contact Lagrangian (CL).

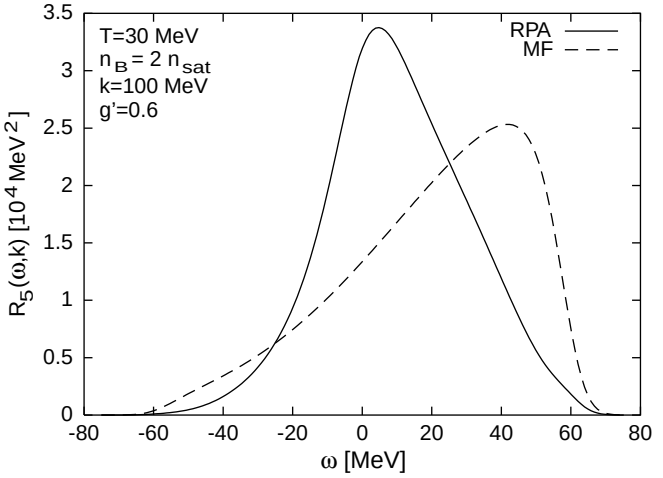

Fig. 3. Structure function R_5, displaying a shift towards lower frequencies.

$\omega^2 < k^2$; moreover, the condition on the scattering angle $-1 < \cos\theta < 1$ imposes that $k^2 < (2E_\nu - \omega)^2$. The integration range is therefore restricted to $k \in [0, \infty[$ and $\omega \in [-k, \min(k, 2E_\nu - k)]$ or, equivalently, $\omega \in [-\infty, E_\nu]$ and $k \in [|\omega|, 2E_\nu - \omega]$.

The RPA correction to the transverse polarization is mostly determined by the ρ-meson, whereas the σ and ω mesons contribution to this quantity remains small. An example of the shape of the transverse structure function is displayed in fig. 2 in the mean-field approximation (full line) and with RPA corrections included (dashed line). The results of fig. 2 were obtained for a density twice that of saturation, a temperature 30 MeV and at a fixed value of the 3-momentum 100 MeV.

We find that the dependence in the Landau-Migdal parameter g' is very small, when it is introduced through a contact Lagrangian (CL), in contrast with the results reported in [13,17]. The dashed line representing our RPA result is unchanged at the level of precision of the figure whether we take $g' = 0.6$ or $g' = 0$. This discrepancy probably has to be traced to the fact that the latter references are using Horowitz's ansatz (HA). Indeed, when the π-ρ mixing and the components of the $G_\pi^{\mu\nu}$ tensor orthogonal to q^μ, generated by the inversion of eq. (19), are kept in the equations, we would obtain the dotted line of fig. 2 represented for $g' = 0.6$. These terms actually would dominate over the other contributions from the ρ-meson, and would be responsible for a strong suppression of the transverse response function. They are proportional to g'. As was argued in the preceding section and in [39] however, these contributions are spurious and should be subtracted. Once these components are removed, the results of Horowitz's ansatz coincide exactly with those of the contact Lagrangian (CL). We believe that this point needs to be investigated further.

The strong g'-dependence of the transverse response observed by the authors of [13,17] was also at the origin of the large reduction factors with respect to the mean-field results obtained in the RPA approximation in these references. A further consequence of our results is therefore that we expect only a moderate modification of the RPA results with respect to the mean field.

We believe that it makes sense that the introduction of a residual interaction to correct the behavior of the pion propagator, should not dramatically affect the final result, since it was seen from (27),(28) that the pion itself does not contribute to neutrino-nucleon scattering at this level.

Figure 3 shows the structure function R_5 for the same conditions of temperature, density and exchanged momentum as in the two previous figures. The RPA correlations shift this response function towards lower frequencies. Whereas the longitudinal response R_1 was suppressed, this contribution is enhanced. If the unphysical components of the pion propagator were kept, one would again obtain a strong g'-dependence; nevertheless, when they are removed or when the calculation is performed using the contact Lagrangian ansatz, the dependence of the result on g' is so small that it is not apparent on the scale of the figure.

As discussed in the previous section, the polarizations entering the definition of the dressed meson propagators in the RPA approximation contain a contribution from the vacuum fluctuations which needs to be renormalized. At the present time, there exist some discrepancies in the literature concerning the choice of a renormalization procedure. As discussed, *e.g.*, in [38,39], this is a source of uncertainty in the determination of the dispersion relations of the mesons in the framework of hadronic models, and in particular in the prediction of the behavior of the effective ρ-meson mass in the medium. We refer the reader to [38–40,43,44] for details. Before we proceed, it is necessary to know in what measure does this issue affect the results presented in this work. Accordingly, we calculated the response functions in three cases. A first

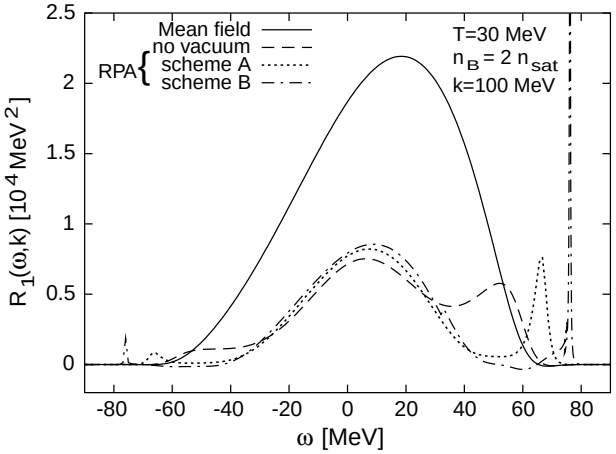

Fig. 4. Effect of renormalization scheme on longitudinal structure function.

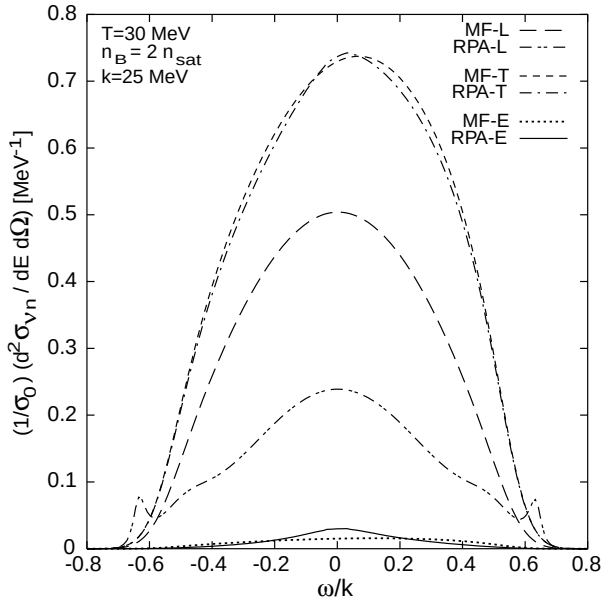

Fig. 5. Relative contributions of longitudinal, transverse and axial-vector polarizations to the differential scattering cross-section.

case consists in simply dropping the vacuum term (which is equivalent to perform a normal ordering). In the second case, ("scheme A" in this work) we chose a renormalization scheme as used by Kurasawa and Suzuki [43], which minimizes the coupling to counterterms on the $q^2 = 0$ shell. In the third case, we used a renormalization procedure which preserved the formal structure of the expressions of the vacuum polarizations as a function of the effective nucleon mass ("scheme 3" of [38]; we will refer to it as "scheme B" in this work).

The choice of the renormalization procedure has some small influence on the longitudinal R_1 response function. As seen from fig. 4, its main effect is to modify the strength and position of the zero-sound mode. It was argued above, however, that the contribution of the zero sound mode to the neutrino-nucleon scattering is only marginal, since its characteristic frequency lies mostly outside of the kinematically allowed values for neutrino-nucleon scattering. Moreover, as will be seen in the next subsection, the longitudinal response is not the dominant contribution to the neutrino-nucleon scattering. The structure functions R_2 and R_5 are not appreciably affected by the choice of the renormalization scheme. The difference between one or the other schemes are of the order of the fraction of a percent and therefore not distinguishable on the scale of the figures. As a consequence, we are able to conclude that the vacuum fluctuations will not affect the neutrino-nucleon scattering opacity in any appreciable way.

3.2 Differential cross-section

The differential cross-section can now be calculated from eq. (7) by inserting the previous results for the longitudinal, transverse and axial-vector polarizations. It is instructive to compare the relative magnitude of their contributions, which are displayed in fig. 5. The result is rescaled by dividing it by the textbook estimate $\sigma_0 = G_F^2 \left(C_V^2 + 3C_A^2\right) E_\nu^2/\pi$ [45]. The transverse contribution is dominant and will provide for about 60% of the total result. We find that it is very little modified by RPA correlations. The corrections arise from the subdominant longitudinal and axial-vector polarizations Π_L and Π_E. The longitudinal contribution is affected by a reduction factor of about two. We notice at the right and left ends of the figure two small peaks which arise from the zero-sound mode excitation. The contribution of the axial-vector response function is only marginal at the density ($n_B = 2\, n_{\rm sat}$) chosen in this figure, although it is larger at higher density. It is slightly enhanced by RPA correlations and its strength is shifted towards lower values of the energy loss of the neutrino $\omega = E_\nu - E'_\nu$, thus acting to counterbalance the reduction from the longitudinal contribution.

As a conclusion to this preliminary study, we gather here the main results of the section. We are able to report that the choice of renormalization scheme does not affect the results more than on the level of less than 1 %. A second important point is that our results are also insensitive to the strength of the residual contact (Landau-Migdal) interaction, in contrast to the findings of other authors. As a consequence, the transverse response function is left almost unchanged by RPA correlations, while the longitudinal and axial-vector responses are reduced by about a factor of two. Since the transverse structure function yields the dominant contribution to the neutrino-nucleon scattering, we do not expect dramatic modifications from RPA correlations as compared to the mean-field result.

4 Full model —asymmetric nuclear matter

Up to now, we have made the simplifying assumption of pure neutron matter. We now pass to describe a more

realistic model, where the proton fraction is defined by the physical conditions in the star. The proton fraction is defined by

$$Y_p = \frac{\rho_p}{\rho_p + \rho_n}\,, \tag{38}$$

where ρ_p and ρ_n are the proton and neutron densities. Numerical calculations show that the chemical equilibrium is reached very rapidly. The proton fraction will therefore be determined by β equilibrium. As a rule of thumb, in cooled neutron stars, the neutrinos can leave the star unhindered, and we have $Y_p \simeq 0.1$. On the other hand, in supernovae the neutrinos are still trapped dynamically inside the matter on the diffusion time scale, and contribute to displace the equilibrium to higher ratios of the proton fraction $Y_p \simeq 0.3$.

The asymmetry enters at several levels in the calculation of the neutrino-nucleon scattering cross-section. It first enters in the determination of the thermodynamics: we have $k_{Fp} \neq k_{Fn}$, and also $M_p \neq M_n$ in a model with δ meson exchange. It also enters in the polarizations, *e.g* we must sum the proton and neutron contributions in polarizations such $\Pi_\sigma = \Pi_\sigma^{(nn)} + \Pi_\sigma^{(pp)}$. Moreover, new mixing channels occur which are not present in symmetric matter. They arise from polarizations involving vertices with mesons of different isospin, which are given by the difference between the proton and neutron contributions, such as, *e.g.*, $\Pi_{\sigma\rho} = \Pi_{\sigma\rho}^{(pp)} - \Pi_{\sigma\rho}^{(nn)}$ in longitudinal modes or $\Pi_{\omega\rho} = \Pi_{\omega\rho}^{(pp)} - \Pi_{\omega\rho}^{(nn)}$ in transverse modes.

4.1 Thermodynamics

The basic properties of nuclear matter can be reproduced at the mean-field level with σ, ω and ρ meson exchange, when non-linear sigma-meson couplings $1/3bm\sigma^3 + 1/4c\sigma^4$ are taken into account in order to obtain a better value of the compressibility (see, *e.g.* [46]).

The δ-meson also appears in meson exchange models such as the Bonn potential [47,48]. Since the δ-meson carries isospin, it can give important contributions in strongly asymmetric matter. Moreover, when density-dependent mean-field models are adjusted in order to reproduce the most recent Dirac-Brueckner-Hartree-Fock calculations, it is seen that a δ-meson is needed in order to reproduce the results at finite asymmetry [49,50]. The behavior of the equation of state when a δ-meson is present was studied by Kubis and Kutschera [51]. The δ-meson is at the origin of a difference between the neutron and the proton effective masses:

$$M_n = m - g_\sigma\sigma + g_\delta\delta\,, \qquad M_p = m - g_\sigma\sigma - g_\delta\delta\,. \tag{39}$$

On the other hand, it brings a negative contribution to the asymmetry energy, so that the coupling to the ρ-meson has to be readjusted to a higher value to compensate for this effect.

In this work, unless stated otherwise, the strength of the δ coupling g_δ will be fixed to the Bonn potential value [47] $g_\delta^2/4\pi = 1.1075$. The couplings g_σ, g_ω, g_ρ, b, c were adjusted [40] so as to reproduce the experimental saturation point with

$$\rho_0 = 0.17\ \text{fm}^{-3}, \quad B/A = -16\ \text{MeV}, \quad K = 250\ \text{MeV}, \quad m_*/m = 0.8, \quad a_A = 30\ \text{MeV} \tag{40}$$

and take the values

$$g_\sigma = 8.00, \quad g_\omega = 7.667, \quad b = 9.637\ 10^{-3}, \quad c = 7.847\ 10^{-3}, \quad g_\rho = 4.59\,. \tag{41}$$

The ratio $\kappa_\rho = f_\rho/g_\rho$ was fixed to the Bonn value $\kappa_\rho = 6.1$.

The proton fraction is determined by the β equilibrium condition $\hat{\mu} = \mu_n - \mu_p = \mu_e - \mu_\nu$. If neutrinos are trapped inside matter, the chemical potential of the neutrino has a finite value $\mu_\nu = (6\pi^2\rho Y_\nu)^{1/3}$. For a typical value of the lepton fraction $Y_L = Y_\nu + Y_e = 0.4$, μ_ν is of the order of 200–250 MeV and the proton fraction Y_p of the order of ~ 0.3–0.36. Y_L is determined by neutrino transport (*e.g.*, diffusion equation), to which the neutrino-nucleon cross-section serves as input. If the matter is transparent to neutrinos, $\mu_\nu = 0$ and the proton fraction is of the order of ~ 0.1. The following figure (fig. 6) show the behavior of thermodynamical parameters relevant for the calculation of the neutrino opacities.

The neutron star matter is assumed to be in β equilibrium. The two cases of neutrino free matter ($Y_\nu = 0$) or matter with trapped neutrinos ($Y_L = 0.4$) are displayed. All figures were drawn assuming a vanishing temperature. The upper left panel shows the evolution of the proton fraction as a function of the baryon density. The upper right panel shows the behavior of the proton and neutron effective masses. The difference $M_p - M_n$ is larger in neutrino free matter since it allows for a smaller proton fraction and therefore a larger mean δ field. On the lower panel are represented the difference between the chemical potentials of the neutron and the proton $\hat{\mu}$ in the cases $Y_\nu = 0$ and $Y_L = 0.4$ as a full line. In matter with a trapped lepton fraction $Y_L = 0.4$, the neutrino chemical potential is non-vanishing; it is compared to $\hat{\mu}$ in fig. 6(c). The full line was obtained for a coupling to the δ field $g_\delta = 5$. If this coupling is set to zero, the chemical potentials are given by the dashed lines in fig. 6(c).

4.2 Meson mixing

The dispersion relations of the σ-ω-δ^0-ρ^0 system of neutral mesons, which is the relevant one for the calculation of the neutrino-nucleon scattering through the neutral-current process, were studied in [40]. As discussed in this reference, the difference existing between the neutron and proton distribution functions makes mixing possible in all channels in asymmetric matter. The pion does not mix with the other mesons and, as pointed out in sect. 3, its contribution to the ν-N scattering process vanishes, so we will not consider it further. The RPA correction is now

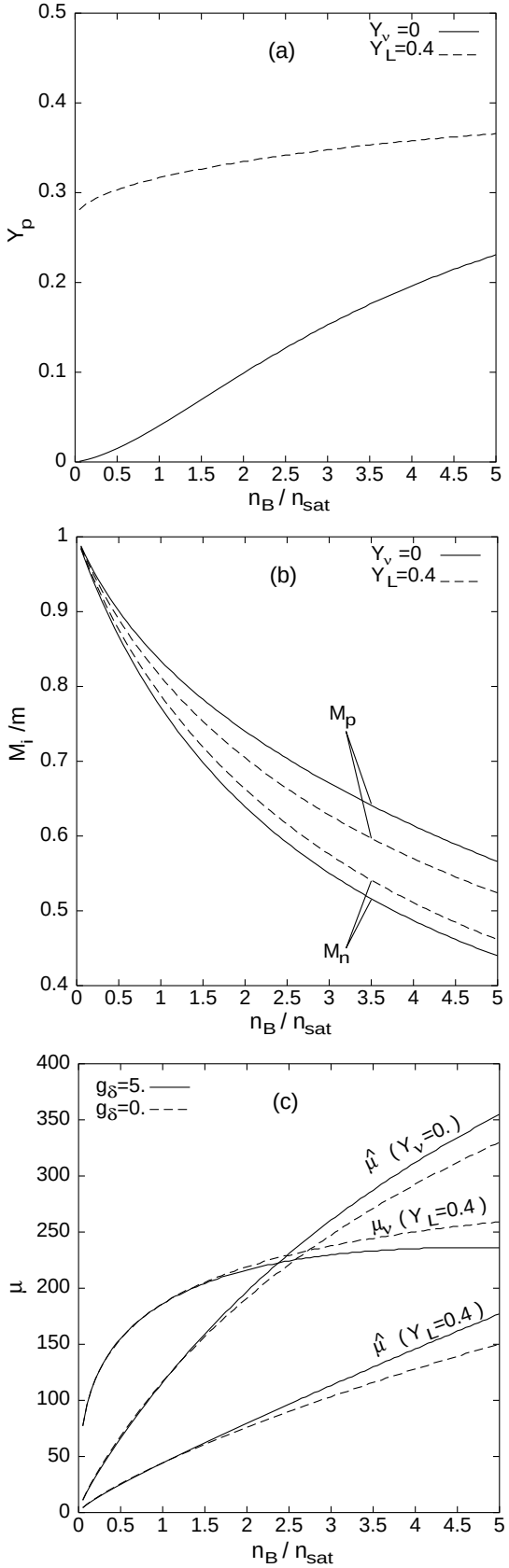

Fig. 6. Thermodynamical parameters in neutron star matter in β equilibrium, both neutrino free ($Y_\nu = 0$) or with trapped neutrinos ($Y_L = 0.4$)

obtained from

$$\Delta\Pi^{\rm RPA} = \left(\Pi_{WS}^{(\sigma)\mu} \quad \Pi_{WS}^{(\omega)\mu\alpha} \quad \Pi_{WS}^{(\delta)\mu} \quad \Pi_{WS}^{(\rho)\mu\alpha}\right) \times \begin{pmatrix} G^{\sigma} & G_{\beta}^{\sigma\omega} & G^{\sigma\delta} & G_{\beta}^{\sigma\rho} \\ G_{\alpha}^{\omega\sigma} & G_{\alpha\beta}^{\omega\omega} & G_{\alpha}^{\omega\delta} & G_{\alpha\beta}^{\omega\rho} \\ G^{\delta\sigma} & G_{\beta}^{\delta\omega} & G^{\delta\delta} & G_{\beta}^{\delta\rho} \\ G_{\alpha}^{\rho\sigma} & G_{\alpha\beta}^{\rho\omega} & G_{\alpha}^{\rho\delta} & G_{\alpha\beta}^{\rho\rho} \end{pmatrix} \times \begin{pmatrix} \Pi_{SW}^{(\sigma)\nu} \\ \Pi_{SW}^{(\omega)\beta\nu} \\ \Pi_{SW}^{(\delta)\nu} \\ \Pi_{SW}^{(\rho)\beta\nu} \end{pmatrix} . \quad (42)$$

Explicit expressions for the dressed meson propagator matrix were given in [40]. The calculation proceeds as in sect. 3. The longitudinal projection of the RPA correction to the polarization now receives contributions from the δ-meson and from all possible combinations of the mixings, that is, not only from σ-ω and δ-ρ already present in symmetric matter, but also from δ-σ, σ-ρ, ω-ρ and ω-δ mixings. The transversal T and axial-vector E components receive additional contributions from ω-ρ mixing. Finally, the projection parallel to $q^\mu q^\nu$, which would contain the contribution of the pion, vanishes through contraction with the (massless) lepton current.

The expressions of $\mathcal{I}m\ (\Pi_R{}^{\mu\nu} L_{\mu\nu})$ so obtained are introduced in the formula for the differential cross-section (7). We calculated separately the longitudinal, transverse and axial-vector contributions to the differential cross-section, and represent them in fig. 7 as a function of the ratio of the neutrino loss energy to the transferred three-momentum $k = 50$ MeV. The thermodynamical conditions were chosen to be those of neutrino free matter ($Y_\nu = 0$) with a density $n = 4\, n_{\rm sat}$ and finite temperature $T = 20$ MeV. The transferred 4-momentum is subject to kinematical constraints which restrict the range over which it will be integrated in order to obtain the total cross-section and the mean free path (see next section). The limit of the integration range is also represented in fig. 7.

The results of the mean-field approximation are represented by the solid line and those of the RPA with full mixing, as described by eq. (42), are represented by the dotted line. In order to illustrate the effect of the meson mixing, we have plotted for comparison the result which would correspond to taking into account the mixing only in the channels that are already open in symmetric matter (*i.e.*, σ-ω and δ-ρ), and setting the other mixings to zero (*i.e.*, σ-ρ, δ-ω, ω-ρ and σ-δ), as has been considered by some authors. This approximation is represented by the dashed line. It can be seen from these figures that the contribution of the longitudinal polarization is appreciably affected by meson mixing.

The longitudinal modes involve the full σ-ω-δ-ρ mixing. The mixing is stronger at high asymmetry and high density. There exists as before a zero-sound mode, but it is indiscernible on the figures, because it is partially washed out by Landau damping and lies outside of the integration range.

The transverse and axial-vector contributions involve only ρ-ω mixing in the transverse modes. The modification of the transverse contribution is small in the kinemat-

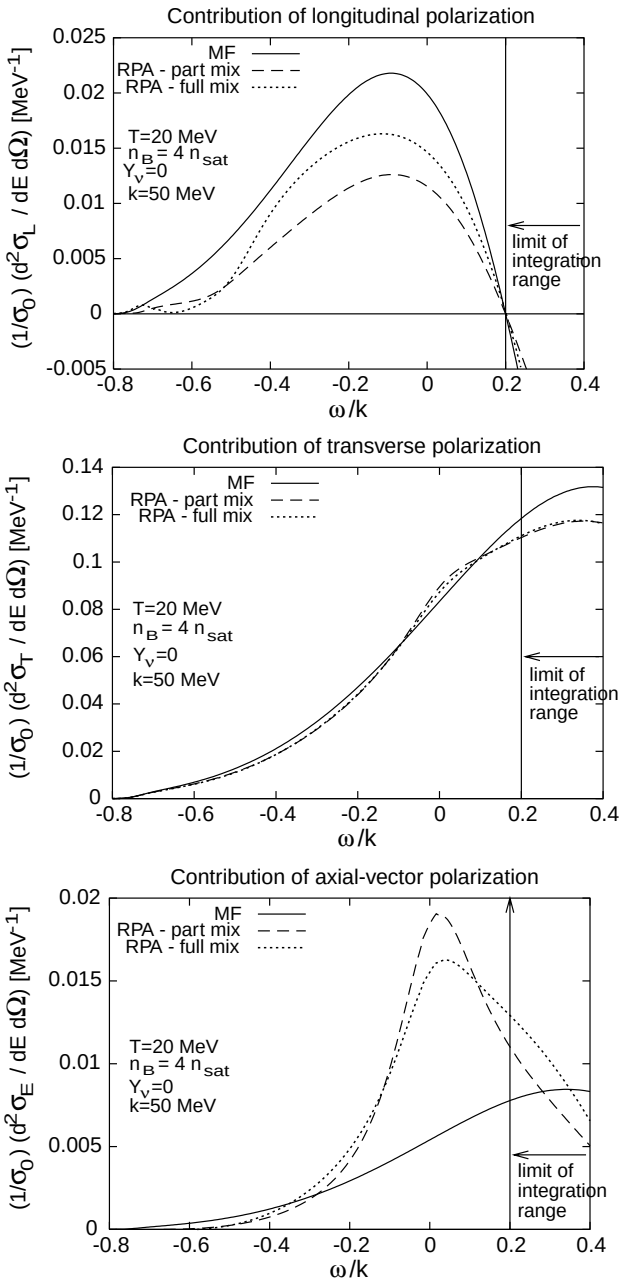

Fig. 7. Contribution of longitudinal (upper panel), transverse (central panel) and axial-vector (lower panel) polarizations to the differential scattering cross-section, showing the correction arising from fully taking into account meson mixing.

ically allowed region. On the other hand, the axial-vector response function is somewhat enhanced by ρ-ω mixing.

The conclusions that were already presented from the preliminary study are confirmed in this more elaborate model. We obtain that the dominant contribution to the neutrino-nucleon scattering cross-section, that is the transverse one, is hardly modified by the RPA corrections as compared to the mean-field approximation. The RPA corrections affect the longitudinal and axial-vector components, the longitudinal part being suppressed and the axial part enhanced with respect to the mean-field approximation, and partially canceling each other. The effect of meson mixing is of the order of 20% on both the longitudinal and axial-vector parts, but further act to counterbalance each other. The net result is that we do not expect dramatic corrections to the global result from RPA correlations.

4.3 Mean free path

Finally, we will calculate the contribution of the neutrino-nucleon scattering to the mean free path, since it gives an immediate feeling of the phenomenon of opacity when it is compared with the length scales typical of the star, *e.g.* the star radius or a typical convection length scale. We must of course stress the fact that this is only an estimate. As a matter a fact, several other processes, like neutrino emission and absorption through charged-current, scattering on electrons, bremsstrahlung... contribute to the definition of the actual mean free path.

The mean free path is defined here as the inverse of the total cross-section per unit volume obtained by integrating the differential cross-section calculated in the preceding sections:

$$\frac{1}{\lambda(E_\nu)} = -\frac{G_F^2}{32\pi^2}\frac{1}{E_\nu^2}\int_0^\infty k\mathrm{d}k \times \int_{-k}^{\omega_{\max}} \mathrm{d}\omega\ \frac{(1-f(E'_\nu))}{1-e^{-z}}\ \mathcal{I}m\left(L^{\alpha\beta}\Pi^R_{\alpha\beta}\right)\ , \quad (43)$$

with

$$\omega_{\max} = \min(2E_\nu - k, k)\,.$$

$(1-f(E'_\nu) = (1+\exp[(E'_\nu-\mu_\nu)/T]))$ is a Pauli blocking factor for the outgoing lepton. The chemical potential μ_ν is determined by β equilibrium and by neutrino transport equations (*e.g.*, diffusion equation), which determine the lepton fraction Y_L at a given instant of the proto-neutron star cooling.

In the following figure (fig. 8), we represented the ratio of total cross-sections as calculated in the RPA and mean-field approximations. The chosen thermodynamical conditions are representative of the earlier stage of the cooling, when the neutrinos are still trapped inside the matter (the lepton fraction was chosen to be $Y_L = 0.4$, for typical values of the temperature ($T = 20$ MeV) and density ($n = 4\,n_{\rm sat}$). The neutrino energy was fixed to $E_\nu = 30$ MeV.

At high density, the total neutrino-neutron scattering cross-section is found to be reduced by RPA correlations by a factor (only) $\sim 10\%$ with respect to the mean-field value. When full meson mixing is taken into account, the reduction is even smaller. This value should be compared to the suppression factors of the order of two quoted in recent publications [13,17]. We think that the explanation for this discrepancy probably lies in the treatment of the short-range correlations, as discussed in sect. 3. Further investigation on this issue is needed.

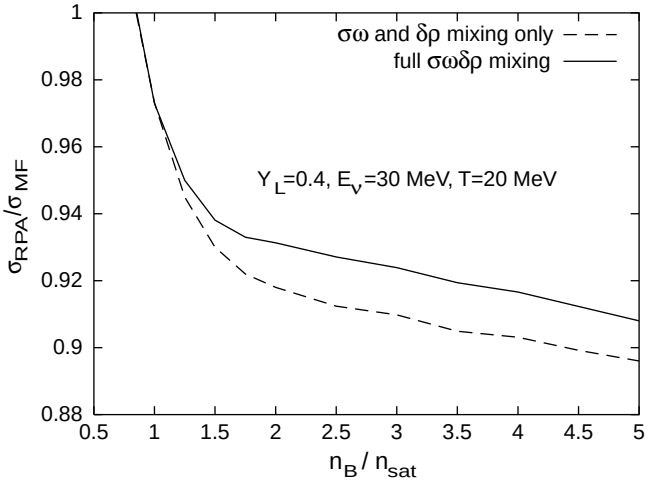

Fig. 8. Reduction factor in matter with trapped neutrinos.

The mean free path obtained from the integration of eq. (43) is shown in fig. 9 in matter with trapped neutrinos as a function of the density for various values of the temperature. At high density, the mean free path is somewhat lengthened by RPA correlations as compared to the mean-field value. At low density and moderate temperature, on the other hand, RPA correlations would yield an enhancement of the cross-section and a reduction of the mean free path. A similar behavior was reported in [17]. It should be kept in mind, however, that the validity of the model becomes questionable in this range.

4.4 Influence of the δ-meson

In this subsection we briefly come back on the role of the δ-meson on the results presented in this work.

The δ-meson affects the neutrino-nucleon cross-section at two levels. First, it introduces a difference between the effective masses of the neutron and the proton. Furthermore, it contributes additional terms to the longitudinal RPA polarization, which are formally similar to those arising from the σ-meson. No additional terms appear in the transverse and axial-vector polarizations.

We studied this contribution by comparing the case where the coupling to the δ-meson is taken to vanish, to the case $g_\delta = 5$. The couplings to the σ and ω fields are given by (41), whereas the coupling to the ρ-meson must be readjusted as follows:

$$(g_\delta = 0.0,\ g_\rho = 3.685)\,, \qquad (g_\delta = 5.0,\ g_\rho = 5.203)\,. \quad (44)$$

(Note that the readjustment of g_ρ necessary to reproduce the asymmetry energy will also indirectly modify the response functions though the polarizations involving the ρ-meson.)

The behavior of the longitudinal, transverse and axial-vector contributions to the differential cross-section are represented in fig. 10 for these two parameter sets. The thermodynamical conditions were taken to be those of matter in β equilibrium with trapped neutrinos at four

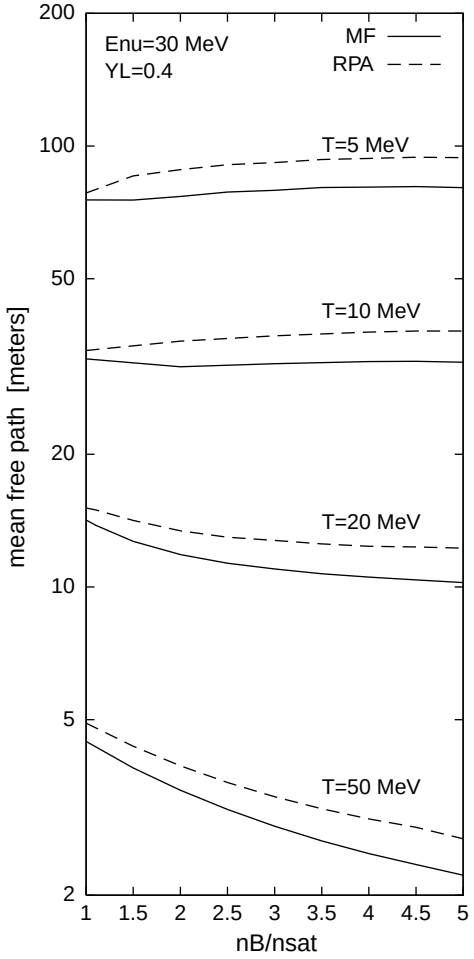

Fig. 9. Mean free path in matter with trapped neutrinos.

times the saturation density and $T = 30$ MeV. The energy of the ingoing neutrino and the transferred momentum were fixed to $E_\nu = 30$ MeV and $k = 100$ MeV. In order to estimate the respective influence of both effects, the artificial case where the mass difference is taken into account, but not the contributions of the δ polarizations, is also represented as a dash-dotted line in the first panel. The coupling to the δ enhances the longitudinal response with respect to the case $g_\delta = 0$, whereas it suppresses the transverse response. The axial-vector response was left practically unchanged. Again, subtle cancellations effects come into play, and prevent us from issuing predictions on the behavior of the total cross-section as a function of g_δ at this stage.

We obtained that the total cross-section, in the conditions of hot and dense matter with trapped neutrinos, was less suppressed with respect to the mean-field value when the coupling to the δ is finite. On the other hand, we realized a calculation for colder ($T = 5$ MeV) and neutrino-free matter, and found in this case the total cross-section to be slightly larger when $g_\delta = 0$ than when $g_\delta = 5$.

5 Summary and perspectives

Let us gather here the main results obtained in this work. Special attention was paid to the issues of renormaliza-

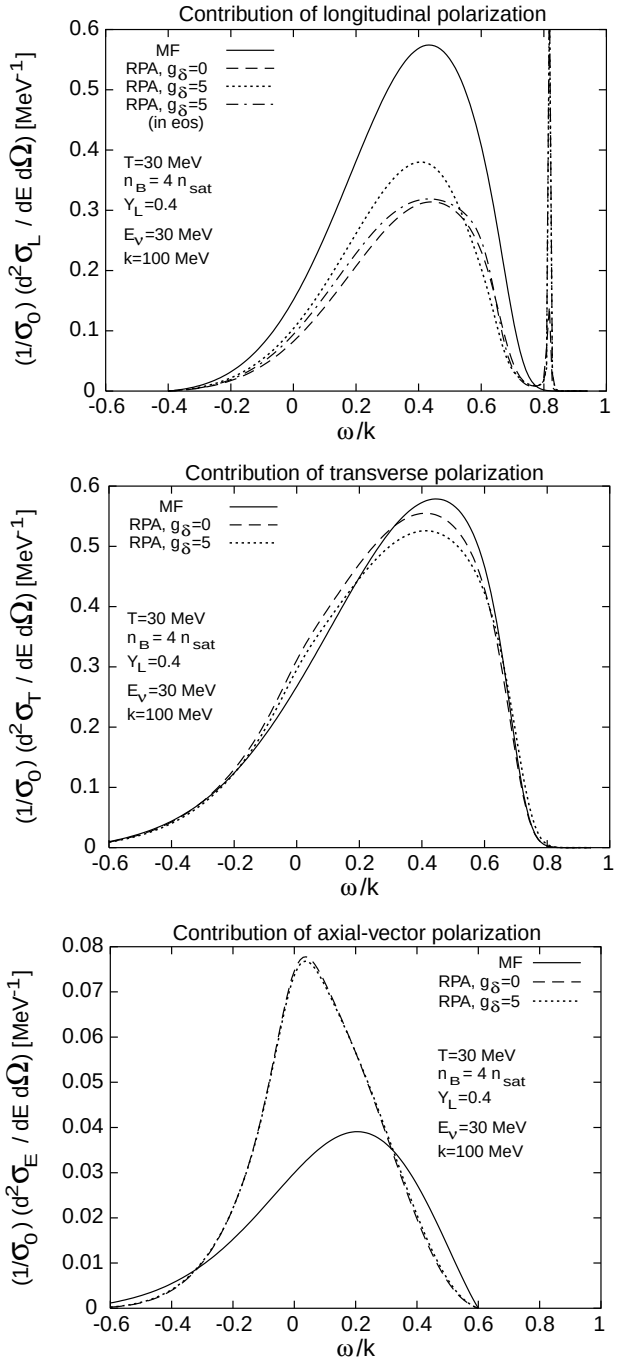

Fig. 10. Influence of the δ-meson on the differential cross-section.

tion of the Dirac sea, residual interactions in the tensor channel, coupling to the δ meson and meson mixing. It has been shown that the vacuum fluctuations have only a negligible effect on the scattering rate. We examined two different prescriptions to modelize short-range correlations, via a Landau-Migdal contact term in the tensor channel. We argue that, when this term is properly handled, it has very little influence on the structure functions, regardless of the value of the parameter g'.

As a consequence, the transverse contribution to the scattering rate is basically unchanged, while the contributions coming from the longitudinal and axial-vector parts combine to produce a 10% to 15% reduction of the scattering rate with respect to the mean field approximation.

These results stay in contrast with the findings of previous authors [13,17], who reported a strong dependence on the strength of the residual interaction. We suggest that the discrepancy originates in the treatment of the ansatz of Horowitz with which this term is usually introduced in the theory, and suggest an alternative ansatz. We believe our result to be consistent with the fact that the unmodified pion does not contribute to the neutral-current process, so that the g' interaction introduced to correct the behavior of the pion propagator should also not drastically affect the final result. Further work is needed to settle this point.

Let us mention at this point that our statement is made for the neutral-current process. We do not expect it to hold for the charged-current processes.

The 10% reduction factor from RPA correlations comes in addition to the reduction effected at the mean-field level by the replacement of the mass and chemical potential of the nucleons by their corresponding effective values in dense matter. The latter reduction depends appreciably on the chosen parameter set, since it regulates the rate of decrease of the effective nucleon mass. We found for example for the set (41) $\sigma_{\rm MF}(M,\mu^*)/\sigma(m,\mu) = 0.75$ in neutrino-free matter at $n = 4\,n_{\rm sat}$, $T = 5\,{\rm MeV}$, $E_\nu = 30\,{\rm MeV}$.

A natural extension of this work concerns the absorption and emission cross-section by the charged-current reaction in the RPA approximation. This is presently under study.

As the density increases, a more complete description should include the hyperons Λ, Σ^-. Taking into account these baryons does not present any particular difficulty, since the structure of the equations is the same, only with different values of the coupling constants. This has been done in [33,52]. As these authors argue moreover, the high fraction of trapped neutrinos and relatively hot temperatures both conspire to strongly suppress the formation of exotic, strangeness-carrying particles, so that these are not expected to have a strong influence on the first few seconds of the life of the proto-neutron star. Nevertheless, the exotica will be determinant on the later stage of the proto-neutron star cooling, at $t \simeq 30$–$60\,{\rm s}$, which are marginally or will soon become observable with the next generation of neutrino detectors now on construction, such as UNO.

A more important problem is to arrive to an accurate description of the short-range correlations. These have been studied separately from RPA corrections by several authors (see, *e.g.* [19,20,23,24]). The calculated correction factors to the neutrino opacities are large, especially in the low density regime. This is in fact related to the well-known problem of nuclear matter descriptions, which should simultaneously take into account short- and long-range corrections, "ladders" and "loops", in a consistent

way. While methods do exist to do so [53], at least in an approximate way, they are quite unwieldy, especially in the relativistic formulation. Some results in this direction have been reported recently in [23].

In matter at subnuclear density, and also at high density, the homogeneous phase may not be the most stable state of matter. It will therefore be important to study the role of ordered configurations, as coherent scattering is expected to dominate in this regime. At low density, and sufficiently low temperatures, the spinodal instability triggers condensation of droplets of a denser phase in a more dilute gas principally composed of neutrons. The droplets take a spatially ordered configuration due to Coulomb forces. This will eventually form the crust of the cooled neutron star. At high density, there are various possibilities of forming ordered structures. For example, if a transition to quark gluon plasma takes place, an important fraction of the matter in the star can be in a mixed phase, and will acquire an ordered structure similar to that present in the crust [46]. Another possibility is the formation of a pion condensate in the alternating spin layer configuration [54]. In any case, such structures are generally unfavored by temperature and high lepton (and proton) fractions, so that the same remark as done before applies: this type of correction is expected to set in at a later phase of the proto-neutron star cooling. It could be very interesting once we are able to detect the tail of the neutrino emission from a supernova event; if a sudden change in the neutrino would occur, it could be interpreted as a signal that a phase transition has taken place.

This work was supported in part by the Spanish Grants nos. MCT-00-BFM-0357, AYA2001-3490-C02-01 and AEN99-0692.

References

1. A. Burrows, J. Goshy, Astrophys. J. **416**, L75 (1993).
2. M. Liebendorfer, A. Mezzacappa, F.K. Thielemann, O.E. Bronson Messer, W.R. Hix, S.W. Bruenn, Phys. Rev. D **63**, 103004 (2001).
3. S.W. Bruenn, Astrophys. J. Suppl **58**, 771 (1985).
4. M. Rampp, H-Th. Janka, Astrophys. J. **539**, L33 (2000).
5. S. Yamada, H.-Th. Janka, H. Suzuki, Astron. Astrophys. **344**, 533 (1999).
6. H.-Th. Janka, Astron. Astrophys. **368**, 527 (2001).
7. A. Habig for the SNEWS collaboration, e-print astro-ph/9912293; K. Scholberg, Nucl. Phys. Proc. Suppl. **91**, 331 (2000); AMANDA collaboration, e-print astro-ph/0105460.
8. N. Iwamoto, C.J. Pethick, Phys. Rev. D **25**, 313 (1982).
9. R.F. Sawyer, Phys. Rev. C **40**, 865 (1989).
10. G. Fabbri, F. Matera, Phys. Rev. C **54**, 2031 (1996).
11. C.J. Horowitz, K. Wehrberger, Phys. Rev. Lett. **66**, 272 (1991); Nucl. Phys. A **531**, 665 (1991).
12. Hungchong Kim, J. Piekarewicz, C.J. Horowitz, Phys. Rev. C **51**, 2739 (1995).
13. S. Reddy, M. Prakash, J.M. Lattimer, J. Pons, Phys. Rev. C **59**, 2888 (1999).
14. S. Reddy, J. Pons, M. Prakash, J.M. Lattimer, *Proceedings of the 2nd Oak Ridge Symposium on Atomic and Nuclear Astrophysics, 2-6 December 1997*, edited by A. Mezzacappa (IOP Publ., 1998) p. 585, e-print astro-ph/9802312.
15. A. Burrows, R.F. Sawyer, Phys. Rev. C **58**, 554 (1998).
16. J. Navarro, E.S. Hernández, D. Vautherin, Phys. Rev. C **60**, 045801 (1999).
17. S. Yamada, H. Toki, Phys. Rev. C **61**, 015803 (2000).
18. G. Sigl, Phys. Rev. D **56**, 3179 (1997).
19. G. Raffelt, D. Seckel, G. Sigl, Phys. Rev. D **54**, 2784 (1996).
20. G. Raffelt, D. Seckel, Phys. Rev. C **52**, 1780 (1995).
21. R.F. Sawyer, Phys. Rev. D **60**, 023002 (1999).
22. S. Yamada, Nucl. Phys. A **662**, 219 (2000)-232.
23. A. Sedrakian, A.E.L. Dieperink, Phys. Rev. D **62**, 083002 (2000).
24. D.N. Voskresensky, e-print astro-ph/0101514.
25. Jiang Wei Zhou, talk given at the *ECT* Conference Physics of Neutron Star Interiors, June 19-July 7, 2000 Trento, Italy.*
26. C.J. Horowitz, J. Piekarewicz, Phys. Rev. C **50**, 2540 (1994).
27. B.D. Serot, J.D. Walecka, *The Relativistic Nuclear Many-Body Problem*, Adv. Nucl. Phys., edited by J.W. Negele, E. Vogt, Vol. **16** (Plenum Press, New York, 1986).
28. See, for example, K. Saito, T. Maruyama, K. Soutome, Phys. Rev. C **40**, 407 (1989); R.J. Furnstahl, B.D. Serot, Phys. Rev. C **44**, 2141 (1991); R.L. Kobes, G.W. Semenoff, Nucl. Phys. B **260**, 714 (1985); **272**, 239 (1986); **260**, 714 (1985).
29. C. Schaab, D. Voskresensky, A.D. Sedrakian, F. Weber, M.K. Weigel, Astron. Astrophys. **321**, 591 (1997).
30. C.J. Horowitz, Nucl. Phys. A **412**, 228 (1984); K. Lim, C.J. Horowitz, Nucl. Phys. A **501**, 729 (1989).
31. H. Kurasawa, T. Suzuki, Nucl. Phys. A **445**, 685 (1985).
32. K. Saito, T. Maruyama, K. Soutome, Phys. Rev. C **40**, 407 (1989).
33. S. Reddy, M. Prakash, J.M. Lattimer, Phys. Rev. D **58**, 013009 (1998).
34. J. Diaz Alonso, Ann. Phys. (N.Y.) **160**, 1 (1985).
35. J. Diaz Alonso, A. Pérez, H. Sivak, Nucl. Phys. A **505**, 695 (1989).
36. J. Diaz Alonso, A. Pérez, Nucl. Phys. A **526**, 623 (1991).
37. E. Gallego, J. Diaz Alonso, A. Pérez, Nucl. Phys. A **578**, 542 (1994).
38. L. Mornas, E. Gallego, A. Pérez, Nucl. Phys. A **699**, 579 (2002) e-print nucl-th/9806093.
39. L. Mornas, e-print nucl-th/0107005.
40. L. Mornas, e-print nucl-th/0107002.
41. R.J. Furnstahl, B.D. Serot, Comments Nucl. Part. Phys. **2**, A23 (2000); R.J. Furnstahl, B.D. Serot, H.-B. Tang, Nucl. Phys. A **618**, 446 (1997).
42. K. Yoshida, H. Toki, Nucl. Phys. A **648**, 75 (1998).
43. H. Kurasawa, T. Suzuki, Nucl. Phys. A **490**, 571 (1988).
44. H. Shiomi, T. Hatsuda, Phys. Lett. B **334**, 281 (1994).
45. S.L. Shapiro, S.A. Teukolsky, *Black Holes, White Dwarfs and Neutron Stars* (Wiley, 1983).
46. N.K. Glendenning, *Compact Stars* (Springer Verlag, 1997).
47. R. Machleidt, K. Holinde, Ch. Elster, Phys. Rep. **149**, 1.
48. R. Machleidt, *The Meson Theory of Nuclear Forces and Nuclear Structure*, Adv. Nucl. Phys., edited by J.W. Negele, E. Vogt, Vol. **19** (Plenum, New York, 1989.)

49. F. de Jong, H. Lenske, Phys. Rev. C **57**, 3099 (1997). C. Fuchs, H. Lenske, H.H. Wolter, Phys. Rev. C **52**, 3043 (1995).
50. H. Shen, Y. Sugahara, H. Toki, Phys. Rev. C **55**, 1211 (1997).
51. S. Kubis, M. Kutschera, S. Stachniewicz, Acta Phys. Polon. B **29**, 809 (1998); S. Kubis, M. Kutschera, Phys. Lett. B **399**, 191 (1997).
52. J.A. Pons, S. Reddy, M. Prakash, J.M. Lattimer, J.A. Miralles, Astrophys. J. **513**, 780 (1999).
53. See, *e.g.*, A.A. Abrikosov, L.P. Gorkov, I.E. Dzyaloshinski, *Methods of Quantum Field Theory in Statistical Physics* (Dover, 1975); M. Bonitz, *Quantum Kinetic Theory* (Teubner Verlag, 1998); A.D. Jackson, T. Wettig, Phys. Rep. **273**, 325 (1994); B.E. Clements, C.W. Greeff, H.R. Glyde, Phys. Rev. B **44**, 5216 (1991), 10239; J.M. Häuser, W. Cassing, A. Peter, Nucl. Phys. A **585**, 727 (1995); J.M. Häuser, W. Cassing, A. Peter, M.H. Thoma, Z. Phys. A **353**, 301 (1996).
54. Prog. Theor. Phys. Suppl. Vol. **112**, issue no. 1 (1993).